

## Thermal-equilibrium relation between the optical emission and absorption spectra of a doped semiconductor quantum well

Toshiyuki Ihara,\* Shun Maruyama, Masahiro Yoshita, and Hidefumi Akiyama

*Institute for Solid State Physics (ISSP), University of Tokyo, 5-1-5, Kashiwanoha, Kashiwa, Chiba 277-8581, Japan*

Loren N. Pfeiffer and Ken W. West

*Bell Laboratories, Alcatel-Lucent, Murray Hill, New Jersey 07974, USA*

(Received 29 June 2009; published 31 July 2009)

We report experimental demonstration of the Kennard-Stepanov (KS) relation, a fundamental equilibrium relation determined by absolute temperature, between photoluminescence (PL) and PL-excitation spectra of a doped quantum well. With the resonant excitation PL measurement technique, the KS relation has been fulfilled at 5–220 K, thanks to the thermal bath provided by the resident carriers introduced with the doping. Crossover to quasi thermal or nonthermal carrier distributions has also been characterized quantitatively via systematic off-resonant excitations.

DOI: [10.1103/PhysRevB.80.033307](https://doi.org/10.1103/PhysRevB.80.033307)

PACS number(s): 78.67.De, 78.55.–m

The Kennard-Stepanov (KS) relation<sup>1–8</sup> connects the linear optical spectra of luminescence  $I(\omega)$  and absorption  $A(\omega)$  for homogeneous luminescent materials under thermal equilibrium. It is expressed by

$$I(\omega)/\omega^2 A(\omega) \propto \exp(-\hbar\omega/k_B T), \quad (1)$$

where  $\hbar\omega$ ,  $k_B$ , and  $T$  are photon energy, Boltzmann's constant, and temperature, respectively. It is an important and useful fundamental relation analogous to Wien's law for blackbody radiation or to the so-called Kubo-Martin-Schwinger (KMS) relation between emission and absorption.<sup>9–12</sup> The KS and KMS relations have been widely used, in both theories<sup>7–12</sup> and experiments in various fields including lasers,<sup>13,14</sup> nanomaterials,<sup>15–17</sup> and biology,<sup>3–6</sup> to derive  $I(\omega)$  from  $A(\omega)$ , or vice versa, when only one of the two is available or much more easily obtained than the other. Moreover, these relations provide a basis for advanced studies of nonequilibrium or hot carrier dynamics.<sup>18</sup> They are also applicable to a temperature measurement standard, or a model-independent noncontact method of evaluating the absolute temperatures of samples or electron systems, particularly in cryogenic environments, where thermal emission is very weak.

However, previous experiments performed to try and verify the KS and KMS relations in various prototypical systems such as dye molecules<sup>3–6</sup> and semiconductors,<sup>15–17</sup> have mostly shown significant disagreements, where they observed deviations from Eq. (1) or  $\omega$ -dependent “spectral” temperatures or obtained inconsistent temperatures much higher or lower than the environmental temperatures depending on the photoexcitation conditions. These were most likely due to inhomogeneity and/or slow thermalization time inherent to such systems, which could hinder one of the important requirements for the KS relation: that excited states must be thermally equilibrated before emission.<sup>3–6</sup> To establish an experimental basis for this useful and important general relation, it is crucial to find a suitable system and examine the experimental possibilities and accuracy in order to confirm the KS relation.

In this Brief Report, we report our study of photoluminescence (PL) and photoluminescence-excitation (PLE) spectra in a modulation-doped quantum well (QW) with a moderate doping density, to examine experimental conditions for realizing the KS relation. We found excellent agreements with the KS relation at various temperatures ranging from 5 to 220 K, indicating excited-state thermal equilibrium, when PL was measured under resonant excitation conditions, where the excitation photon energy is set equal to the PL peak energy. On the other hand, as the excitation energy in PL measurements was changed to the nonresonant regime, we found gradual deviations from the KS relation, especially at low temperatures below 20 K, which suggested the formation of hot or nonequilibrium carrier distributions related to inhomogeneity.

We grew a modulation-doped single QW on a nondoped (001) GaAs substrate by molecular-beam epitaxy. It consisted of the following layers: a 1- $\mu\text{m}$  (GaAs)<sub>9</sub>/(Al<sub>0.36</sub>Ga<sub>0.64</sub>As)<sub>71</sub> superlattice, 6.3-nm GaAs QW, 20-nm Al<sub>0.36</sub>Ga<sub>0.64</sub>As spacer,  $1 \times 10^{11}$  cm<sup>-2</sup> Si delta doping, 450-nm (GaAs)<sub>9</sub>/(Al<sub>0.36</sub>Ga<sub>0.64</sub>As)<sub>71</sub> superlattice, and a 30-nm GaAs cap layer. The electron density in the QW was  $6 \times 10^{10}$  cm<sup>-2</sup> at 4 K. The sample was mounted on a metal cold finger having good thermal conductivity in a continuous-liquid-helium-flow cryostat. The temperature of the cold finger, or the environmental temperature  $T$  of the sample, was controlled using an electric heater and measured with a Si-diode temperature sensor located close to the sample. The accuracy of the sensor was  $\pm 1$  K (1%) at temperatures below (above) 100 K.

Spectra of absorption  $A(\omega)$  and luminescence  $I(\omega)$  were obtained via PLE and PL measurements, in which we excited the sample with a continuous-wave titanium-sapphire laser. The excitation light was focused onto a spot about 2  $\mu\text{m}$  in diameter via an objective lens. PL was collected in a backward-scattering geometry, coupled and dispersed in a 0.75-m spectrometer and then detected with a liquid-nitrogen-cooled charge-coupled-device (CCD) camera having spectral resolution of 0.05 nm. To measure each PLE spectrum, we took PL spectra by scanning the excitation en-

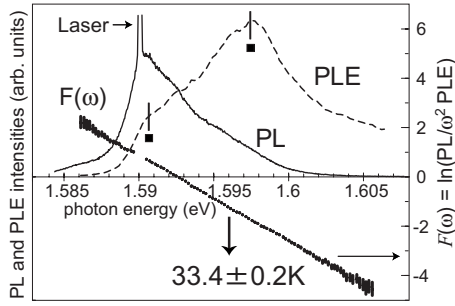


FIG. 1. Normalized PL (solid curve), PLE (dotted curve), and  $F(\omega)$  (vertical line segments) measured at the environmental temperature  $T$  of  $33 \pm 1$  K.

ergies at 100 points with constant steps and plotted all the spectral areas of the respective PL spectra. We minimized the effect of nonlinearity, i.e., dependence of PL spectra on excitation powers, to obtain the spectra in the linear-response regime by reducing the excitation laser power to  $1.7 \mu\text{W}$ . The estimated photoexcited carrier density was less than  $1 \times 10^9 \text{ cm}^{-2}$ . The exposure times for the PL and PLE measurements were set to 60 and 4 s, respectively. All spectra referred to in this Brief Report were measured at the same position on the same sample.

It should be noted that we eliminated intense scattering noise in the excitation light by keeping the sample surface clean, tilting the sample by  $10^\circ$  from the normal plane of the optical axis, setting the polarization of detection perpendicular to that of excitation light, and putting an iris between the objective lens and the spectrometer coupling lens in the detection path. These steps were essential to obtain high signal-to-noise ratios in our particular measurements of PL spectra in the resonant excitation condition, where the excitation energy was set equal to the PL peak energy and of PLE spectra. Note that our PLE measurements plotted the total PL intensities in all the spectral areas, while conventional PLE measurements plot partial PL intensities in only low-energy tails of PL peaks. Our method enables precise PLE spectral measurements, which should directly give access to the optical absorption, even when the PL spectral shapes change with excitation photon energy.

First, we studied PLE and PL measured under the resonant excitation conditions. Figure 1 shows typical results at  $T=33 \pm 1$  K. The dashed curve shows the PLE spectrum, and the solid curve indicates the PL spectrum measured at the excitation energy of 1.590 eV, which is the same as the PL peak energy. Two peaks indicated by solid squares originated from the nonuniformity of the sample, or monolayer (ML) thickness fluctuations. Also shown by vertical line segments in Fig. 1 is  $F(\omega)=\ln[I(\omega)/\omega^2 A(\omega)]$ , where  $I(\omega)$  and  $A(\omega)$  are determined by the PL and PLE spectra, respectively. The length of each vertical segment of  $F(\omega)$  indicates the error bar estimated from the CCD camera noise in both PL and PLE spectra. The data of  $F(\omega)$  in Fig. 1 represent a remarkably straight line with a constant slope against photon energy.

To compare the straight line of  $F(\omega)$  with the KS relation in Eq. (1), we performed line fitting to  $F(\omega)=-\hbar\omega/k_B T^* + C$  taking  $T^*$  and  $C$  as  $\omega$ -independent fitting parameters. For

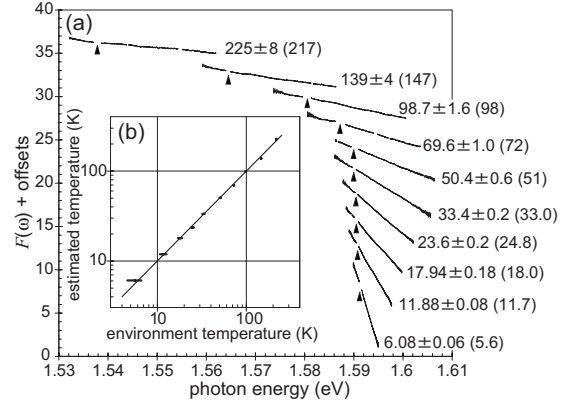


FIG. 2. (a)  $F(\omega)$  measured at various temperatures plotted on each offset. Filled triangles indicate excitation energies set to be resonant to the PL peak energies. Values inside and outside the parentheses indicate  $T$  and  $T^*$ , respectively. (b) Plots of estimated temperatures  $T^*$  as a function of environmental temperatures  $T$ . The solid line indicates  $T^*=T$ .

that, we used the weighted least-squares method,<sup>19</sup> where the phenomenological standard deviation was set to be consistent with the calculated standard deviation. The estimated slope  $1/k_B T^*$  was  $0.347 \pm 0.002 \text{ (meV}^{-1}\text{)}$ , which corresponds to  $T^*=33.4 \pm 0.2$  K. This agreed well with the environmental temperature  $T=33 \pm 1$  K. The KS relation was satisfied rigorously.

Figure 2(a) shows  $F(\omega)$  at various temperatures  $T$  from 5 to 220 K measured in the same way as in Fig. 1. Each result is plotted with an arbitrary offset. Filled triangles indicate the excitation energies for PL measurements set at the PL peak energies under the resonant excitation condition. It is striking that all the  $F(\omega)$  data showed straight lines with constant slopes against photon energy at all temperatures and in all detectable photon energy regions, including not only the higher energy sides but also the lower energy sides of the excitation energies.

Values inside and outside the parentheses in Fig. 2(a) correspond to the temperatures  $T^*$  estimated from the slope of  $F(\omega)$ , and the environmental temperatures  $T$ , respectively. The relation between  $T^*$  and  $T$  is plotted in Fig. 2(b), in which a line indicating  $T^*=T$  is also drawn. Excellent agreements between  $T^*$  and  $T$  were found in these experiments. In short, the KS relation, or Eq. (1), was thoroughly satisfied in a wide range of temperatures for the spectra of resonantly excited PL and PLE.

From these results, we may conclude that, as long as PL was measured under resonant excitation conditions, almost perfect agreements with the KS relation for PLE and PL in the doped QW were observed, which indicates that the excited-state thermal equilibrium was realized. This has a significant impact on the experimental study of the KS relation because such thorough agreements have never been observed in other systems such as intrinsic semiconductor QWs or dye molecules.<sup>3-6,15-17</sup>

Next, we studied the excitation-energy dependence of PL spectra and resulting  $F(\omega)$ . Figure 3 shows the spectra at  $T=33 \pm 1$  K of PLE (a) and of PL with excitation at 1.588 eV (b) and 1.598 eV (c), which are below and above the PL peak

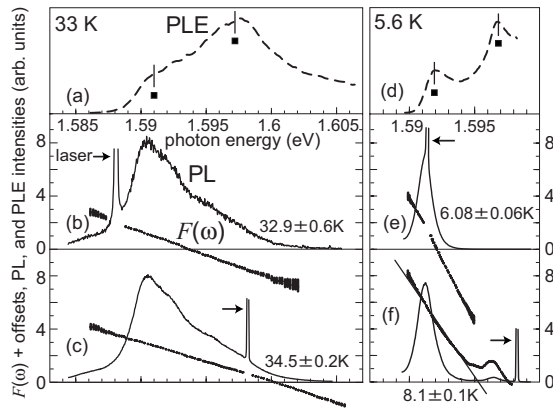


FIG. 3. Normalized PLE, PL spectra, and  $F(\omega)$  measured at 33 K (left a–c) and 5.6 K (right d–f), respectively. We set different excitation energies for the PL in (b) and (c) and for the PL in (e) and (f).

energy, respectively. Corresponding plots of  $F(\omega)$  are shown in (b) and (c), both of which fit straight lines very well. However, the estimated values of  $T^*$  were slightly different:  $32.9 \pm 0.6$  K and  $34.5 \pm 0.2$  K for (b) and (c), respectively. Compared with the case of resonant excitation shown in Fig. 1,  $T^*$  changed by  $-0.5$  K and  $+1.1$  K. These straight lines with  $T^*$  slightly different from  $T$  are one of the typical features of the nonresonant excitation condition.

The right panels (d)–(f) of Fig. 3 show results at  $T = 5.6 \pm 1$  K. In the resonant excitation case shown in Fig. 3(e),  $F(\omega)$  fit a straight line well, and  $T^*$  was  $6.08 \pm 0.06$  K, which was almost the same as  $T$ . However, in the nonresonant excitation case shown in Fig. 3(f),  $F(\omega)$  did not exhibit a straight line. Significant deviation from a straight line was found, in particular at around 1.596 eV, which corresponds to the spectral structure of a 1-ML thinner QW. By fitting the limited data near the PL peak in Fig. 3(f), we obtained  $T^*$  of about  $8.1 \pm 0.1$  K, which was much higher than  $T$ . This deviation from a straight line and the large difference between  $T$  and  $T^*$  are unique features of nonresonant excitation at low temperature.

Figure 4 summarizes  $T^*$  thus obtained as a function of excitation photon energies at various environmental temperatures. The origin of the  $x$  axis at 0 meV indicates resonant excitation. The environmental temperature  $T$  is displayed as a horizontal gray bar with an error bar of  $\pm 1$  K. Except for the region denoted by “partial fit,” each  $T^*$  represented a constant slope of a straight  $F(\omega)$  line, as shown in Figs. 3(b), 3(c), and 3(e). Under near-resonant excitation conditions around 0 meV, we observed a slight and systematic increase in  $T^*$  against excitation energy. These observations indicate the formation of quasi-thermal-equilibrium carrier distributions with hot or cold carrier temperatures  $T^* \neq T$  depending on the excitation photon energies. The gradient of this increase in  $T^*$  was 0.5 K/meV at  $T=5$  K and 0.2 K/meV at  $T=33$  K. Note that the measured  $T^*$  and its gradient did not depend on the excitation laser intensities because all the measurements were done in the weak linear-response regime. Thus, excitation-intensity-dependent heating of the sample or hot phonon accumulations has been negligible.

In the region denoted by partial fit, we observed a clear

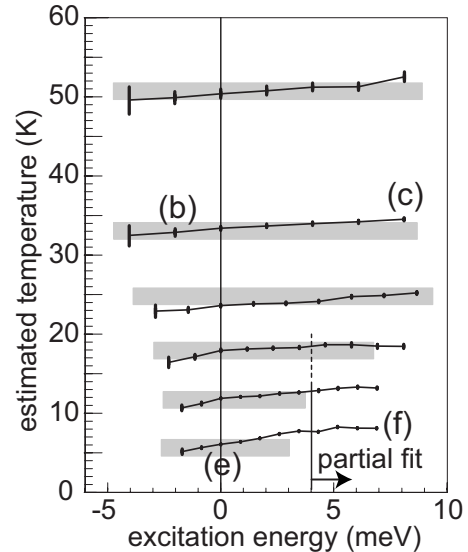


FIG. 4. Plots of  $T^*$  as a function of excitation energy measured at 5–50 K. The indices of (b), (c), (e), and (f) correspond to the measurements shown in Fig. 3.

deviation in  $F(\omega)$  from a straight line, as shown in Fig. 3(f). Such a significant deviation from the KS relation under nonresonant excitation conditions must have originated from the formation of nonthermal carrier distributions. This type of deviation was found at  $T < 20$  K and with excitation energy more than 4 meV higher than resonance. This energy gap of 4 meV is comparable to the 6-meV-higher energy position of the 1-ML thinner QW. This suggests that inhomogeneity was one of the key reasons for the deviation from the KS relation.

Let us now discuss the present results. As long as PL was measured under the resonant excitation condition, almost perfect agreements with the KS relation for PLE and PL in the doped QW were observed, which have never been observed in other systems.<sup>3–17</sup> We interpret these findings as indicating that doping is one of the key factors in realizing the excited-state thermal equilibrium, which relaxed the problem of finite thermalization time against PL lifetime. In the doped QW, the doped majority carriers are in thermal equilibrium with the lattice and their environments, and the minority photoexcited carriers can quickly reach thermal equilibrium with the doped carriers via strong electron-electron interactions. This is not the case with intrinsic semiconductor QWs<sup>15,16</sup> and wires,<sup>17</sup> where the photoexcited carriers must interact directly with the lattice via a slow electron-phonon relaxation rate.

In some previous experiments with molecular systems,<sup>3–6</sup> sample inhomogeneity was a key problem that made it difficult to realize the excited-state thermal equilibrium. Actually, the inhomogeneity also existed in the present sample, as evidenced by the ML terrace peaks marked by solid squares in Figs. 1 and 3. However, such a problem must have been reduced by carrier diffusion or mobility in the QW. We expect the excited-state thermal equilibrium to be realized when the diffusion length of photoexcited carriers is more than the characteristic length of the inhomogeneity, for example, at elevated temperatures. This reasonably explains the observed absence (existence) of ML peak structures in  $F(\omega)$

shown in Fig. 3 and the agreement (disagreement) with KS relation at high (low) temperatures. Moreover, to minimize the inhomogeneity problem, resonant excitation was of great help in a QW because spatially separated ML-thin QW regions with far higher energy participate in PL measurements with high-energy off-resonant excitations, but they do not participate in PL measurements with resonant excitations.

Now, let us discuss possible reasons for the 0.2–0.5 K/meV gradient of  $T^*$  against excitation photon energy that appeared under near-resonant excitation conditions in Fig. 4, and corresponding quasithermal distributions with  $T^* > T$ . Note that the calculated increase in the initial temperature of photogenerated carriers due to excess photon energy is 11.6 K/meV, and the measured gradient is much smaller than this (by a factor of 20–50) and independent of the excitation photon densities. This excludes the possibility of uniform heating of the electron gas and/or lattice to achieve quasiequilibrium because their masses and heat capacities are far larger than those of photoexcited carriers. Instead, the excess energy of photoexcited carrier must have been shared with localized electrons and/or lattice. This is possible, for example, in local quasithermal distributions, where photoexcited carriers share their excess energies with only neighboring localized electrons or puddles in the nonlinear screening regime

formed by the potential inhomogeneity.<sup>20,21</sup> Such a possibility needs to be further investigated in future studies by changing the doping density and sample homogeneity.

Finally, we point out the relevance of the current Brief Report to cryogenic technology and low-temperature basic studies of electron transport and optics because it provides a rare example and a powerful way to directly measure the internal temperature or electron temperature of a semiconductor sample attached to a cold finger in a cryostat without assuming any model and any calibrations.

In summary, we reported an experimental investigation of the KS relation in a doped GaAs QW. Under resonant excitation conditions, we found that the ratio between PL and PLE spectra was determined by only the environmental temperature (5–220 K) in the form of the KS relation. On the other hand, nonresonant excitation caused deviation from the KS relation, which originated from the formation of a quasi equilibrium with hot carrier temperatures or nonequilibrium carrier distributions, especially at low temperatures below 20 K.

This work was partly supported by KAKENHI (Grants No. 20104004 and No. 20360135) of MEXT, Japan.

\*t-ihara@iis.u-tokyo.ac.jp

<sup>1</sup>E. H. Kennard, *Phys. Rev.* **11**, 29 (1918).

<sup>2</sup>B. I. Stepanov, *Sov. Phys. Dokl.* **2**, 81 (1957).

<sup>3</sup>D. A. Sawicki and R. S. Knox, *Phys. Rev. A* **54**, 4837 (1996).

<sup>4</sup>R. Croce, G. Zucchelli, F. M. Garlaschi, R. Bassi, and R. C. Jennings, *Biochemistry* **35**, 8572 (1996).

<sup>5</sup>H. Dau and K. Sauer, *Biochim. Biophys. Acta* **1273**, 175 (1996).

<sup>6</sup>A. Kowski, P. Bojarski, and B. Kukliński, *Z. Naturforsch., A: Phys. Sci.* **54a**, 465 (1999).

<sup>7</sup>R. S. Knox and L. F. Marshall, *J. Lumin.* **85**, 209 (2000).

<sup>8</sup>Y. Zhao and R. S. Knox, *J. Phys. Chem. A* **104**, 7751 (2000).

<sup>9</sup>H. Haug and S. Schmitt-Rink, *Prog. Quantum Electron.* **9**, 3 (1984).

<sup>10</sup>S. W. Koch, T. Meier, W. Hoyer, and M. Kira, *Physica E (Amsterdam)* **14**, 45 (2002).

<sup>11</sup>R. Zimmermann, *Many-Particle Theory of Highly Excited Semiconductors* (Teubner, Leipzig, 1987).

<sup>12</sup>N. H. Kwong, G. Rupper, B. Gu, and R. Binder, *Proc. SPIE*, **6461**, 64610I (2007).

<sup>13</sup>P. Blood, A. I. Kucharska, J. P. Jacobs, and K. Griffiths, *J. Appl. Phys.* **70**, 1144 (1991).

<sup>14</sup>P. Rees and P. Blood, *IEEE J. Quantum Electron.* **31**, 1047 (1995).

<sup>15</sup>S. Chatterjee, C. Ell, S. Mosor, G. Khitrova, H. M. Gibbs, W. Hoyer, M. Kira, S. W. Koch, J. P. Prineas, and H. Stolz, *Phys. Rev. Lett.* **92**, 067402 (2004).

<sup>16</sup>H. W. Yoon, D. R. Wake, and J. P. Wolfe, *Phys. Rev. B* **54**, 2763 (1996).

<sup>17</sup>D. Y. Oberli, F. Vouilloz, R. Ambigapathy, B. Deveaud, and E. Kapon, *Phys. Status Solidi A* **178**, 211 (2000).

<sup>18</sup>J. Shah, *Hot Carriers in Semiconductor Nanostructures: Physics and Applications* (Academic, New York, 1992).

<sup>19</sup>W. H. Press, B. P. Flannery, S. A. Teukolsky, and W. T. Vetterling, *Numerical Recipes in C* (Cambridge University, Cambridge, England, 1988).

<sup>20</sup>M. Yamaguchi, S. Nomura, T. Maruyama, S. Miyashita, Y. Hirayama, H. Tamura, and T. Akazaki, *Phys. Rev. Lett.* **101**, 207401 (2008).

<sup>21</sup>G. Allison, E. A. Galaktionov, A. K. Savchenko, S. S. Safonov, M. M. Fogler, M. Y. Simmons, and D. A. Ritchie, *Phys. Rev. Lett.* **96**, 216407 (2006).